Strategy of Search and Refinement by GA in 2-D Photonic Crystals with Absolute PBG

Gilliard Nardel Malheiros-Silveira, Vitaly Félix Rodríguez-Esquerre, and Hugo E. Hernández-Figueroa, *Senior Member, IEEE*

***Abstract*— The finite element method (FEM) and the genetic algorithm (GA) have been used to solve the inverse problem involving absolute photonic band gap (PBG) searching and optimization. Square and triangular lattices composed by Tellurium (anisotropic material) and air have been analyzed. In order to avoid the requirements of high computational efforts and resources needed in these kind of tasks, the PBGs have been computed only at key positions along the first region of Brillouin and we obtained absolute midgap ratio, considering PBGs between the TE 1–2 and TM 3–4 modes, of 18.00% and 23.49% for the square and triangular lattices, respectively.**

***Index Terms*— Anisotropic optical materials, finite element method, genetic algorithms, photonic band gap, photonic crystals.**

I. Introduction

ABSOLUTE band gaps in a two-dimensional Photonic Crystal (PC) results when both polarization modes exhibits superposition of their forbidden band gaps (i.e., polarization independent). In any PC the search and optimization of absolute PBGs are obtained by exploring their parameters: lattice type, filling factor, refractive indexes, shape and through the symmetry reduction.

In [1] and [2], triangular and square lattices of dielectric rods of Tellurium in air are analyzed and total PBGs were obtained by changing the filling ratio.

The isolated and combined effects of the symmetry reduction and air hole introduction in the crystal elements have been studied in Tellurium in [3].

Recently, [4] explored the absolute PBG maximization, in annular photonic crystals [5], by using also Tellurium in square, triangular and honeycomb lattices and considering several geometries inside the crystals (circular, triangular, elliptical, rectangular and square).

In all the cases, the Plane Wave Expansion (PWE) method has been used. However, in-plane light propagation down 2-D PCs was investigated in [6] and [7] by using the FEM in frequency domain and the calculated results showed a good agreement when compared to the results obtained by the PWE. While the PWE is a full-matrix method and therefore highly time consuming for complex geometries, it is well known, that the FEM is a very flexible and efficient numerical technique to model devices/components with inhomogeneous and complex structures. Furthermore, the FEM, compared to the Finite Difference Time Domain Method (FDTD), exhibits convergence of the same order and has no modeling limitations for highly inhomogeneous structures.

In this work, we also explored PC composed by Tellurium and air in both lattices (square and triangular) and we considered the inverse problem. We have considered the use of Tellurium in order to compare our optimization strategy with previously published results [1], [2] and [4]. In this way we have obtained PCs with optimized absolute PBGs. GA have been used for this purpose because of their proved capabilities to solve these kinds of problems [8]–[10]. In order to compute the PBGs a FEM based formulation [6], [11] and [12] has been used.

Although there are not many photonic applications involving the Tellurium, recently, a compact Polarization Beam Splitter (PBS) using PC, composed by Tellurium, with absolute PBG has been investigated [13]. (To realize a multimode PC waveguide based PBS, both TE and TM polarizations must propagate with low loss in the structure.)

Expressive results have been obtained here and they are superior to those previously published. Although the proposed strategy has been applied to obtain absolute PBGs in anisotropic materials, the same can also be applied for simpler problems such as the isotropic case and also for only one polarization.

In next section, an introduction about PBG computing and the implementation of the GA in conjunction with the FEM will be presented, then, numerical results and the optimized geometries will be discussed and the main conclusion of this work will be given at the end.

II. Methods

A. Photonic Band Gap

The two used lattices can be seen in Fig. 1, in both cases, just for simplicity, they are represented by circular elements inside the unitary cell. In order to obtain the PBG we just need to analyze the unitary cell imposing appropriated

Manuscript received July 5, 2010; revised October 13, 2010; accepted October 17, 2010. Date of current version March 9, 2011. This work was supported by CNPq Process 302390/2009-0, 305992/2005-8, CAPES, INCT FOTONICOM/CNPq/FAPESP.

G. N. Malheiros-Silveira and H. E. Hernandez-Figueroa are with the Department of Microwaves and Optics, School of Electrical and Computer Engineering, University of Campinas, São Paulo 13083-97, Brazil (e-mail: gilliard@dmo.fee.unicamp.br; hugo@dmo.fee.unicamp.br).

V. F. Rodriguez-Esquerre is with the Department of Electrical Engineering, Federal University of Bahia, Salvador 40210-630, Brazil (e-mail: vitaly@pq.cnpq.br).

Digital Object Identifier 10.1109/JQE.2010.2091107

0018–9197/$26.00 © 2011 IEEE

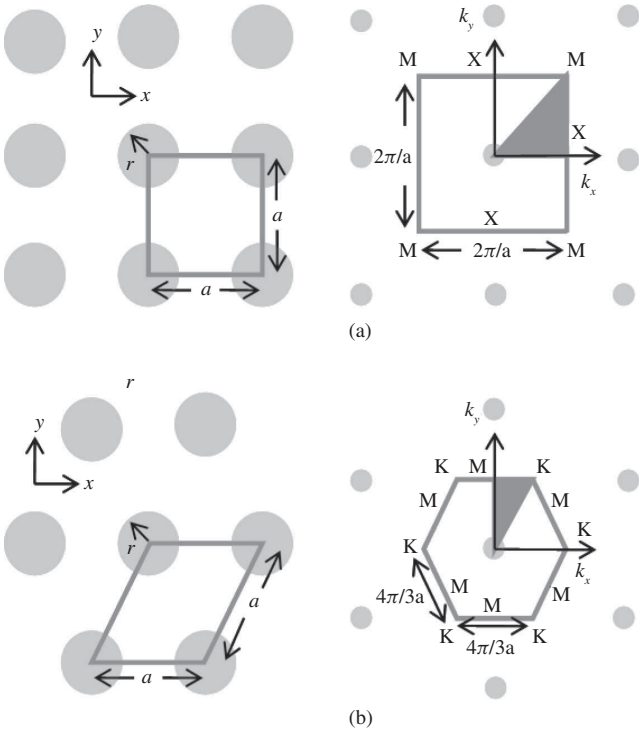

Fig. 1. Two-dimensional lattices and Brillouin zones. (a) Square lattice and its correspondent Brillouin zone. (b) Triangular lattice and its correspondent Brillouin zone.

boundary conditions by using the frequency domain 2-D FEM approach [6], [11] and [12]. The FEM analysis of 2-D PCs can be treated separately for the TM modes and TE modes. In both cases we start from the second order wave equation given by,

$$-\frac{\partial}{\partial x}\left(p\frac{\partial \Phi}{\partial x}\right)-\frac{\partial}{\partial y}\left(p\frac{\partial \Phi}{\partial y}\right)=q\left(\frac{\omega}{c}\right)^2\Phi, \tag{1}$$

where, $p = 1/n_o, q = 1$ and $\Phi = E_z$ for TE modes and $p = 1$, $q = n_e$ and $\Phi = H_z$ for TM modes. Here, n_o and n_e are the ordinary and extraordinary refractive indexes of Tellurium, respectively. The fields E_z and H_z can be written as

$$E_z = \mathrm{e}_z e^{-jk_x x}e^{-jk_y y}, \tag{2a}$$
$$H_z = h_z e^{-jk_x x}e^{-jk_y y}, \tag{2b}$$

where e_z and h_z are the fields' spatial envelopes and k_x and k_y are the propagation constants in the x and y direction, respectively. Substituting (2) in (1), applying the conventional Galerkin method [6], and discretizing the computational domain using 6-node isoparametric second-order triangular elements [6] we obtain an eigenvalue problem given by,

$$[A]\{\varphi\}=\left(\frac{\omega}{c}\right)^2[B]\{\varphi\}, \tag{3}$$

where the vector $\{\phi\}$ is the e_z or the h_z field. For TE modes, matrices $[A]$ and $[B]$ are given by,

$$\begin{aligned}[A] = \sum_e \Bigg[&\iint_e \frac{1}{n_o^2}\frac{\partial\{N\}}{\partial x}\frac{\partial\{N\}^T}{\partial x}\partial x\partial y \\ &+\iint_e \frac{1}{n_o^2}\frac{\partial\{N\}}{\partial y}\frac{\partial\{N\}^T}{\partial y}\partial x\partial y \\ &+jk_x\iint_e \frac{1}{n_o^2}\left(\frac{\partial\{N\}}{\partial x}\{N\}^T-\{N\}\frac{\partial\{N\}^T}{\partial x}\right)\partial x\partial y, \\ &+jk_x\iint_e \frac{1}{n_o^2}\left(\frac{\partial\{N\}}{\partial y}\{N\}^T-\{N\}\frac{\partial\{N\}^T}{\partial y}\right)\partial x\partial y \\ &+\iint_e \frac{1}{n_o^2}\left(k_x^2+k_y^2\right)\{N\}\{N\}^T\partial x\partial y\Bigg]\end{aligned} \tag{4}$$

$$B = \sum_e \iint_e \{N\}\{N\}^T\partial x\partial y. \tag{5}$$

For TM modes, matrices $[A]$ and $[B]$ are given by,

$$\begin{aligned}[A] = \sum_e \Bigg[&\iint_e \frac{\partial\{N\}}{\partial x}\frac{\partial\{N\}^T}{\partial x}\partial x\partial y \\ &+\iint_e \frac{\partial\{N\}}{\partial y}\frac{\partial\{N\}^T}{\partial y}\partial x\partial y \\ &+2jk_x\iint_e \frac{\partial\{N\}}{\partial x}\{N\}^T\partial x\partial y \\ &+2jk_x\iint_e \frac{\partial\{N\}}{\partial y}\{N\}^T\partial x\partial y \\ &+\iint_e \left(k_x^2+k_y^2\right)\{N\}\{N\}^T\partial x\partial y\Bigg],\end{aligned} \tag{6}$$

$$B = \sum_e \iint_e n_e^2\{N\}\{N\}^T\partial x\partial y. \tag{7}$$

Because of the periodicity of the crystalline structure we only discretize one unitary cell and periodical boundary conditions are applied by making equal the fields at the top and the bottom, and the fields at the left and right sides of the unitary cell. The values of k_x and k_y are restricted to the first Brillouin region. (see Fig. 1)

In order to obtain the PBG for asymmetric structures, we need to solve the problem at the labeled points in the first Brillouin zone. See Fig. 1.

The shaded areas are used for problems with folded symmetry and they are limited by $\Gamma(0,0)\pi/\mathrm{a}$ $-\mathrm{X}(1,0)\pi/\mathrm{a}$ $-\mathrm{M}(1,1)\pi/\mathrm{a}$ $-\Gamma(0,0)\pi/\mathrm{a}$ e $\mathrm{M}(0,2\sqrt{3}/3)\pi/\mathrm{a}$ $-\Gamma(0,0)$ π/a $-\mathrm{K}(2/3,2\sqrt{3}/3)$ π/a $-\mathrm{M}(0,2\sqrt{3}/3)\pi/\mathrm{a}$, for the square and triangular lattices, respectively. In the inverse problem considered here, the inner configuration of the unitary cell (material disposition) has been considered to present the most arbitrary geometry. In such a case we need to solve at all the labeled points because maximum and minimum frequencies lies in those points. Consequently we have to compute the PBG at nine

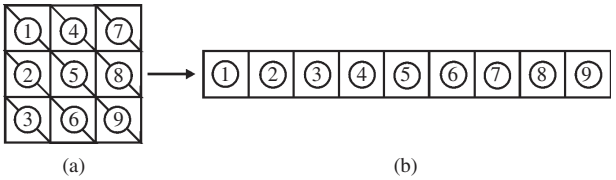

Fig. 2. Codification of the problem. (a) Unitary cell discretized using 18 triangular elements. (b) Chromosomic representation of the unitary cell using 9 genes, each one composed by two triangle elements connected by their hypotenuse.

and at thirteen points if the lattices are square or triangular, respectively.

We considered absolute PBGs in Tellurium for comparison purposes with previously published results [1], [2] and [4], where the same material as here was used. Absolute PBGs have been obtained here by using uniaxial anisotropic Tellurium which has two values of refractive index: $n_e = 6.2$ (extraordinary) and $n_o = 4.8$ (ordinary) for wavelengths between 3.5μm and 35μm. The extraordinary axis has been considered to be along the z axis [1] and [2].

B. Genetic Algorithm

GA is a meta-heuristic method inspired in the natural selection theory. It works with an initial population of candidate solutions represented by chromosomes and the problem parameters are in their genes. Along generations, genetic operators are applied to the chromosomes: selection, crossover, mutation and elitism. In this way, better individuals or solution of the problem are expected in each generation. More details can be found in [14].

The binary codification has been adopted here due to the nature of the search space (mesh). In this way, each pair of triangles (of the mesh), represents one gene on the chromosome, whose alleles are represented with "0's" (air is present) or "1's" (Tellurium is present). The codification is represented in Fig. 2, for the square lattice, with 3x3 mesh. For the triangular lattice the same representation is used.

The main flux of the GA adopted here is represented in Fig. 3(a), where the search strategy and optimizations are represented in Fig. 3(b). The GA was implemented using Matlab®.

The details and main characteristics of the GA operators presented in Fig. 3 (a) are explained in details:

Initial Population: All the individuals of the first step (*global search*) are generated randomly. In the next step (*local optimization*) the first generations is composed by clones of the best individual of the previous step, but using now a refined mesh, resulting in chromosomes with much more number of genes. But before the fitness computation, in this new step all the clones, except one, are mutated.

Fitness: The fitness function is obtained by the intersection of the PBG of some TE and TM modes of the PC. The PBG for the TE 1–2 and TM 3–4 modes are first obtained, and the absolute PBG is obtained by using the function given by:

$$f = \frac{E_{top} - E_{bottom}}{E_{middle}} \times 100\% \tag{8}$$

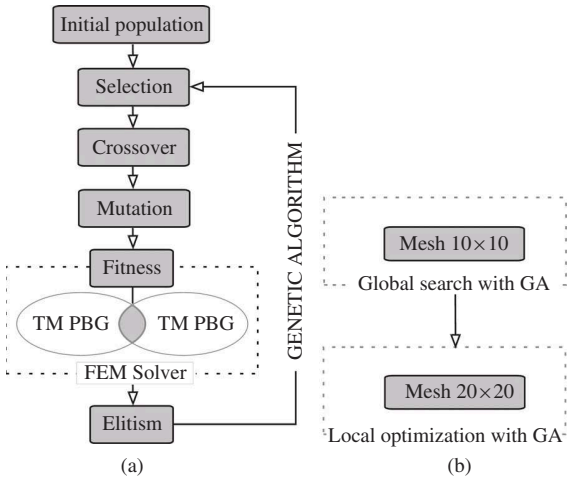

Fig. 3. (a) Flowchart of the GA. (b) Strategy refinement.

where E_{top}, E_{bottom} and E_{middle} mean the lower frequency of the higher mode, the upper frequency of the lower mode and the average of these two previous frequencies, respectively. In this way the fitness function is obtained by the intersection of the PBGs of the TE 1–2 and TM 3–4 modes. In this process the FEM solver is called twice, each call solves and returns the PBG of each polarization. The TE 1–2 and TM 3–4 modes were chosen for comparison purposes. The mode calculation is done by using a FEM based solver written in FORTRAN [6], [11] and [12].

Selection: the selection method was the *roulette-wheel*, and repeated pairs were eliminated and replaced for other pair. Observe that a pair of chromosomes can exhibit the same fitness, because they can represent the same geometry with a rotation of 90°, 180° and 270°.

Crossover: This operator is applied in two random points with a random distance between them. Consequently, we expect a higher diversity of individuals in all the generations.

Mutation: in both steps, *global search* and *local optimization*, this operator affects only one gene chosen randomly in each chromosome.

Elitism: We preserve the best present individual, which must be present in future generations.

A flowchart of the proposed search and refinement strategy based in GA is shown in Fig. 3(b), where the initial process begin with an execution of GA (Fig. 3(a)) in a 10×10 rectangular mesh, this step is called *global search*. When the *global search* is finished, after meeting a stop criterion, we start the *local optimization* by using a refined mesh (20×20). The generations will be now composed by the best individuals and their mutant clones. In this step, the mutation operator is applied in all the generations and in all the individuals, except for one at the first generation, to guarantee the convergence.

A more detailed version of the flowchart shown in Fig. 3(b) is represented by a scheme with a fictitious situations (and considering only one chromosome) shown in Fig. 4 (where "a" represents the lattice constant).

The absolute PBG search process is initially performed by considering a uniformly discretized unitary cell of the crystal (chromosome) by using 200 second order triangular elements,

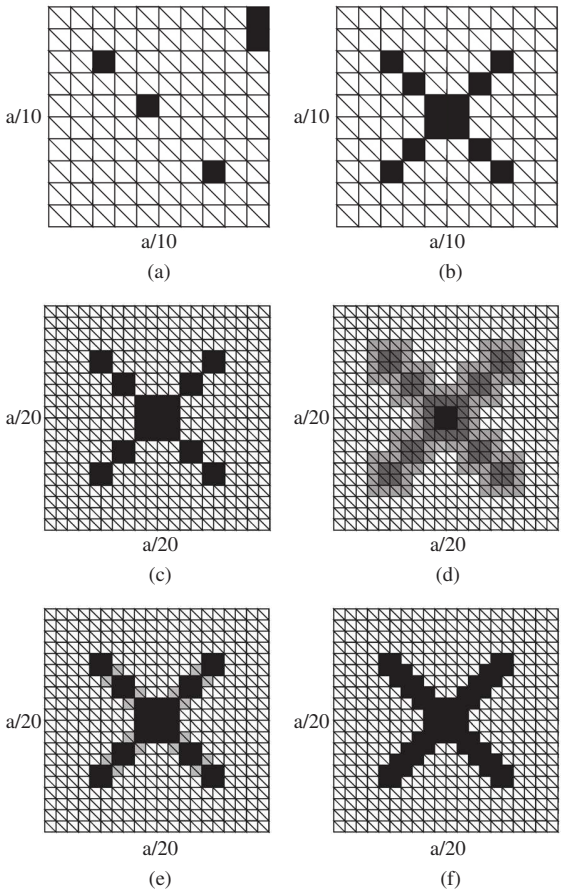

Fig. 4. Strategy of search and refinement by GA. (a) and (b) represent an individual of the initial population and the best individual at the end of the first step (*global search* with a mesh 10×10), respectively. (c) and (d) represent individuals in the second step (*local optimization*). (c) is the best individual of the previous run projected in a mesh 20×20; (d) the shaded region contains the possible genes that can suffer mutation; (e) the light gray regions represent the local where mutation happened and resulted in an increasing of the absolute PBG by refining the 10×10 structure; and (f) represents the optimized unitary cell.

where each square is formed by two triangles representing one gene the chromosome. The process begins with a 10×10 mesh (100 genes) such that each gene is filled with one type of material (Fig. 4(a)).

Initially, a *global search* is performed, where the stop criterion adopted for this case study is the obtaining of higher fitness values than those reported in [2] (Fig. 4(b)). Next, a new run will be performed considering the initial population composed by clones of the best individual of the previous run and the unitary cell is discretized by using a finer mesh composed by 800 second order triangular elements (or 400 genes) (Fig. 4(c)). At this point the *global search* is substituted by a *local optimization* and the mutation operator is applied at the boundary regions between dielectric material and air by removing or adding dielectric material (Fig. 4(d)). It has been implemented a function that recognizes the genes corresponding to the boundary elements. Considering the previous step (Fig. 4(c)), light gray regions (Fig. 4(d)) are susceptible to addition of materials and dark gray regions (Fig. 4(d)) to removal of one. The dark gray and light gray regions change dynamically from one to another generation being redefined in each generation, and each chromosome.

The optimal alterations promoted in previous step (Fig. 4(d)) are shown in Fig. 4(e) (light gray regions) and the optimized unit cell (considering a new stop criterion) is shown in Fig. 4(f).

The mutation operator, is applied only in shaded region represented in (Fig. 4(d)), and is applied to all the individuals in all generations.

The *local optimization*, in the way that has been applied, it decreases the search space and results in less computation time for the optimization. Additionally, it allows the final structure to be composed of agglomerated materials avoiding isolated regions with small fraction of material, reducing, consequently, the fabrication process commonly used.

If only two materials are considered, previously published results suggest that the resulting geometries will be composed by materials in an agglomerated way [9]. This idea has been incorporated in the first generation (of the *global search*) to obtain the initial population, and through the limited search space to mutation operator at *local optimization*.

TABLE I
COMPUTATION TIME OF THE FEM SOLVER AS A FUNCTION OF THE NUMBER OF GENES

	Search Space	Average time in FEM Solver (Eq. 1)	
		Square Lattice	Triangular Lattice
Mesh 10×10	2^{100}	5.5 s	7.3 s
Mesh 20×20	2^{400}	13.4 s	19.6 s
Mesh 40×40	2^{1600}	52.6 s	77.9 s

III. NUMERICAL RESULTS AND DISCUSSION

The computational platform used was a Laptop with Intel ® Core™ 2 Duo processor T7300 (2.0GHz, 800MHz FSB, 4MB L2 cache), RAM 4GB with Windows XP. The average computation time corresponding to the FEM solver as a function of the number of genes in the chromosome is presented in Table I for the computation of 6 eigenvalues over the nodes of the first Brillouin region.

We considered the existence of absolute PBGs between the TE 1–2 and TM 3–4 modes. The band gap calculation has been performed in 9 and 13 points of the first Brillouin region for the square and triangular lattices, respectively. The above consideration reduces significantly the computational efforts and processing time. At the end of the optimization process we verified the value of the optimized PBG by computing the band gap over more points and a mesh 40×40 to corroborate de results of the FEM. The obtained results for square and triangular lattices are presented in next section. For the two study cases here analyzed the population size, and the genetic operators: selection, crossover, mutation and elitism, remain unaltered in the two steps.

A. Square Lattice

The evolution of the fitness as a function of the number of generations as well as the resulting unitary cell are shown in

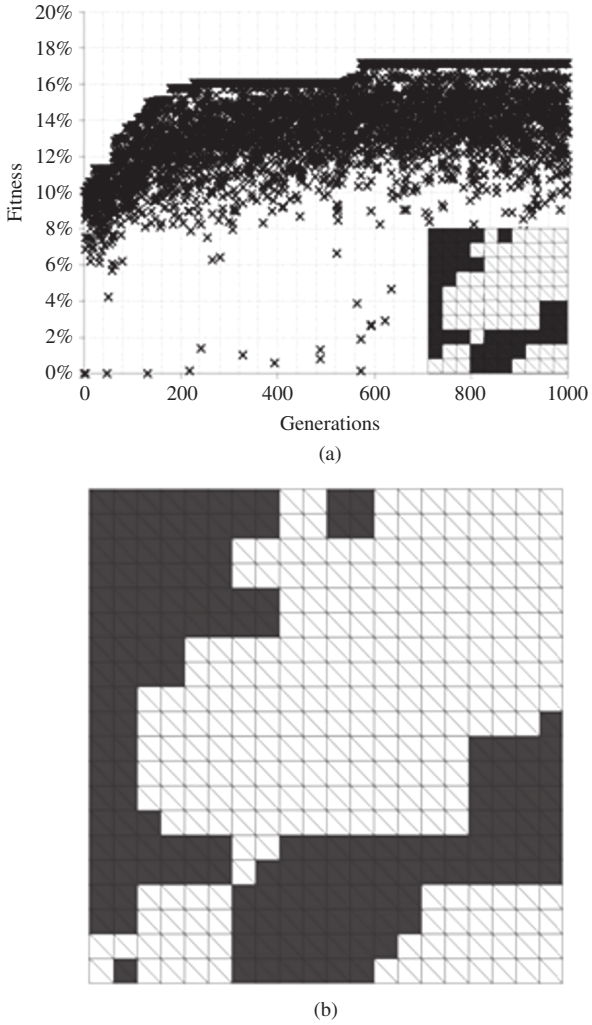

Fig. 5. (a) GA convergence and better structure (inset) of the unit cell with mesh 10×10. (b) Optimized structure for mesh 20×20 (the black cells are formed by Tellurium and white by air).

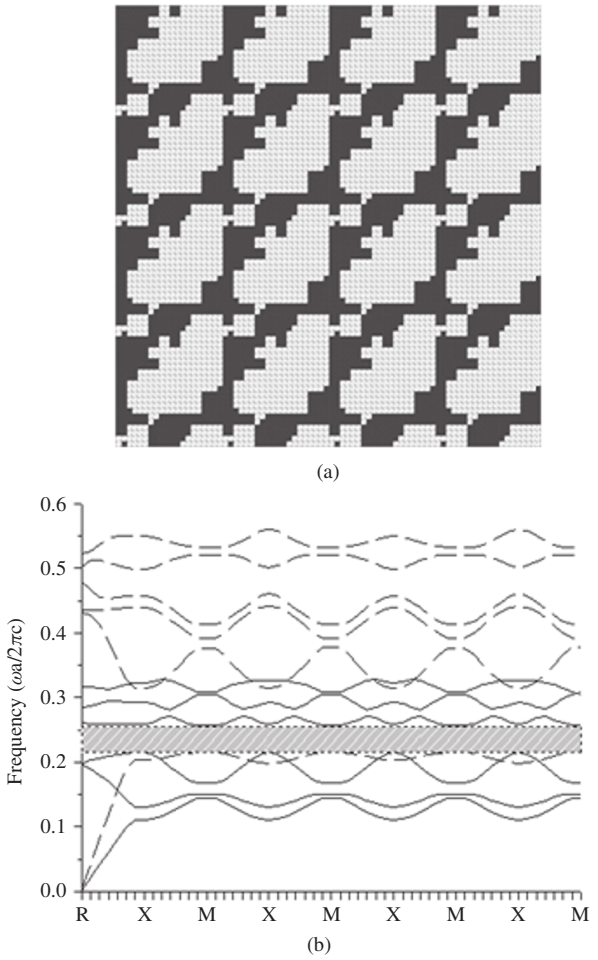

Fig. 6. (a) Crystalline structure corresponding to the unit cell of Fig. 5 (b). (b) Dispersion relation (TE modes in solid lines and TM modes in dashed lines).

Fig. 5(a). Each generation is composed by six individuals and it is observed that the composition of population presenting original PBG has favored the evolution of the algorithm as a whole. A large diversity of individuals with different fitness is also observed; which indicates that there was a reasonable exploration of the *global search*, also characterized by individuals of low fitness. The configuration of the unit cell obtained for the square arrangement on a mesh 10×10 is shown as an inset in Fig. 5(a). On the other hand, most of the individuals exhibit a good fitness. It can be attributed to the coarse discretization of the unitary cell. In Fig. 5(b), we can observe the resulting optimized geometry when a finer mesh is used (20×20).

The optimized crystal is shown in Fig. 6(a). The dark areas are Tellurium. The dispersion diagram of this structure can be seen in Fig. 6(b). A comparison with previously published results is shown in Table II. Here, the convergence of the results is confirmed when the crystal obtained by optimizing on a mesh 20×20 is compared with a mesh 40×40. The PBG for the TM mode is almost twice the PBG of the TE mode as shown in Fig. 6(b).

TABLE II
ABSOLUTE PBGS OPTIMIZED BY GA TO SQUARE LATTICE

Ref.	PBG (2πc/a)	midgap ratio (%)
[2]	$\Delta\omega = 0.037$	$\Delta\omega/\omega_g = 15.20$
[4]	$\Delta\omega = 0.0673$; 0.402-0.469	$\Delta\omega/\omega_g = 15.44$
This Study	$\Delta\omega = 0.0426$; 0.215-0.258	$\Delta\omega/\omega g = 17.14$ (mesh 10×10) $\Delta\omega/\omega g = 18.01$ (mesh 20×20) $\Delta\omega/\omega g = 18.00$ (mesh 40×40)

B. Triangular Lattice

In a similar fashion, we present the results corresponding to the triangular lattices. The evolution of the fitness as a function of the number of generations as well as the resulting unitary cell are shown in Fig. 7(a). We can realize a similar behavior for the evolution if compared with the square lattice. In Fig. 7(b), we can observe the resulting optimized geometry when a finer mesh is used (20×20).

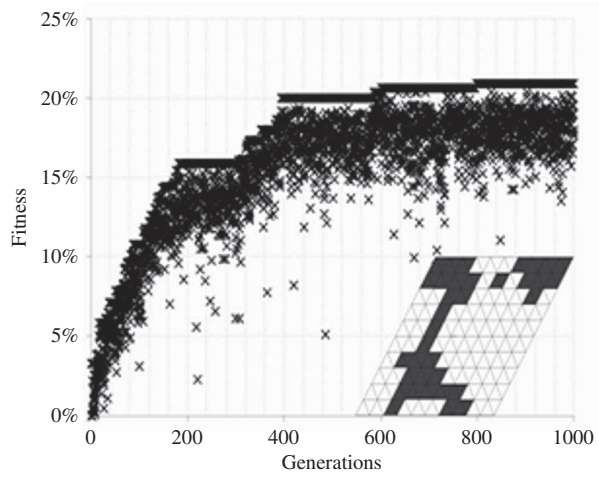

(a)

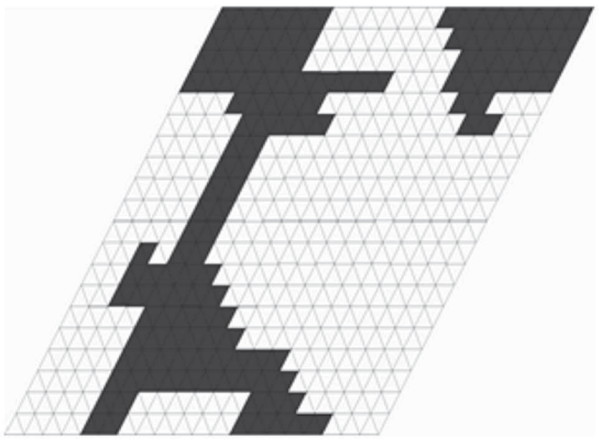

(b)

Fig. 7. (a) GA convergence and better structure (inset) of the unit cell with mesh 10×10. (b) Optimized structure for mesh 20×20 (the black cells are formed by Tellurium and white by air).

TABLE III
ABSOLUTE PBGS OPTIMIZED BY GA TO TRIANGULAR LATTICE

Ref.	PBG (2π c/a)	midgap ratio (%)
[2]	$\Delta\omega = 0.046$	$\Delta\omega/\omega_g = 18.00$
[4]	$\Delta\omega = 0.0959$; $0.415 - 0.511$	$\Delta\omega/\omega_g = 20.72$
This Study	$\Delta\omega = 0.0627$; $0.235 - 0.298$	$\Delta\omega/\omega g = 20.89$ (mesh 10×10) $\Delta\omega/\omega g = 23.49$ (mesh 20×20) $\Delta\omega/\omega g = 23.49$ (mesh 40×40)

The optimized crystal is shown in Fig. 8(a). The dark areas are Tellurium. The dispersion diagram of these structure can be seen in Fig. 8(b). A comparison with previously published results is shown in Table III. Here, the convergence of the results is confirmed when the crystal obtained by optimizing on a mesh 20×20 is compared with a mesh 40×40. The PBG for the TM mode is almost twice the PBG of the TE mode as observed in Fig. 8(b).

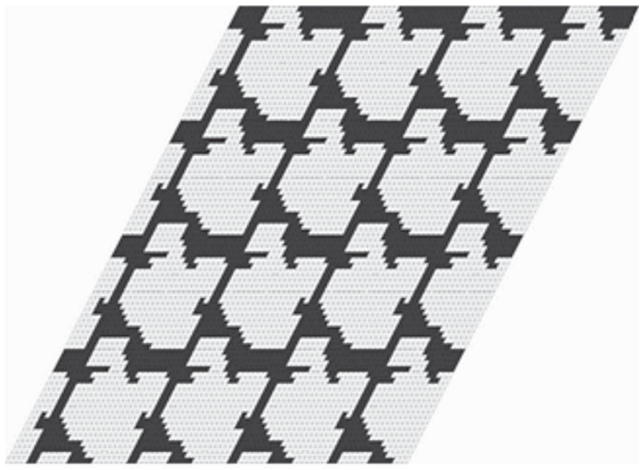

(a)

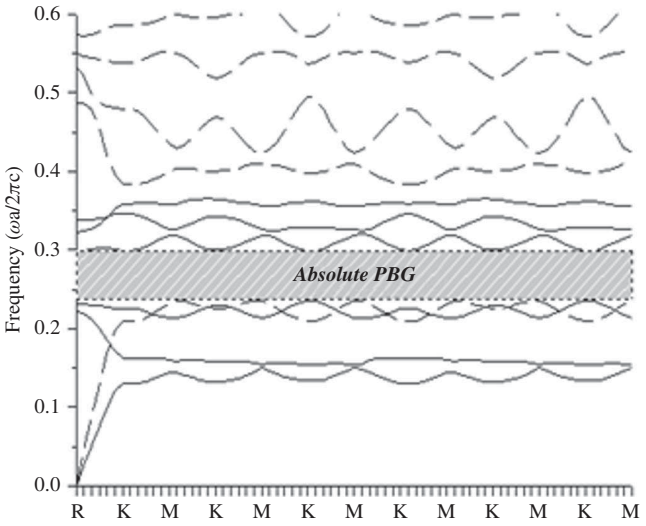

(b)

Fig. 8. (a) Crystalline structure corresponding to the unit cell of Fig. 7 (b). (b) Dispersion relation (TE modes in solid lines and TM modes in dashed lines).

In our study, the resulting optimized geometries can be considered as being air regions in Tellurium in an opposite way as suggested in [1] and [2], where absolute PBGs can be found easily in geometries composed by considering Tellurium dielectric rods in air.

It has been adopted a refining strategy by optimizing first a unitary cell divided in 200 triangles. In both analyzed cases, square and triangular lattices, the GA search produces better results than previously published ones in less than 1000 generations as can be seen in Tables II and III. The resulting geometry is then used in order to start the optimization of the unitary cell using a finer mesh composed by 800 triangles; for this process we fixed a maximum of 200 generations. Although the values obtained by using more elements showed an increment of the absolute PBG, the same can be considered small. It can be explained because the small contribution of smaller elements.

As mentioned in Section II, the mutation operator changes only one gene per chromosome, this permits to explore a search space larger and more feasible. In addition, it covers the possibilities of settings if they have more genes involved in this step simultaneously.

The resulting geometries, given in Fig 6(a) and Fig 8(a), are asymmetric. The same behavior can be seen in [3], where Tellurium PCs with a filling factor lower than 0.3 exhibits larger PBGs when its symmetry is reduced.

The resulting nontrivial structures, differently of circles and ellipses, which are the most traditional ones analyzed, become the fabrication process more complex. However, if we use PBGs in higher order modes, the constant lattice become bigger and the robustness and fabrication tolerance can be improved. In this work we treat PBGs in lower order modes for comparison purposes with previously published results [1], [2] and [4].

It can be expected that the proposed refining strategy can arrive to better results in other cases involving inverse problems where known structures should be optimized, e.g. optimizations involving superprism effects, switching and splitters.

Although the proposed strategy has been applied to the optimization of absolute PBGs in anisotropic materials, the same can also be applied in problems considering only one polarization. In the problems analyzed here, only one refinement has been considered for the square and triangular lattice.

IV. Conclusion

We presented the band gap optimization of PCs composed of Tellurium and air by using the FEM in conjunction with the GA. The square and triangular lattices have been considered and the resulting geometries can be considered as being air holes in Tellurium, contrasting with previous published results. One limitation of the obtained geometries is the difficult to be produced if compared with dielectric rods of Tellurium in air or air holes in Tellurium substrate. However, this limitation can be overcome if the PBG is designed for operating at lower frequencies where the lattice constant is increased.

References

[1] Z.-Y. Li, B.-Y. Gu, and G.-Z. Yang, "Large absolute band gap in 2-D anisotropic photonic crystals," *Phys. Rev. Lett.*, vol. 81, no. 12, pp. 2574–2577, Sep. 1998.

[2] Z.-Y. Li, B.-Y. Gu, and G.-Z. Yang, "Improvement of absolute band gaps in 2-D photonic crystals by anisotropy in dielectricity," *Eur. Phys. J. B*, vol. 11, no. 1, pp. 65–73, Sep. 1999.

[3] R. P. Zaccaria, P. Verma, S. Kawaguchi, S. Shoji, and S. Kawata, "Manipulating full photonic band gaps in 2-D birefringent photonic crystals," *Opt. Exp.*, vol. 16, no. 19, pp. 14812–14820, Sep. 2008.

[4] B. Rezaei, T. F. Khalkhali, A. S. Vala, and M. Kalafi, "Absolute band gap properties in 2-D photonic crystals composed of air rings in anisotropic tellurium background," *Opt. Commun.*, vol. 282, no. 14, pp. 2861–2869, Jul. 2009.

[5] H. Kurt and D. S. Citrin, "Annular photonic crystals," *Opt. Exp.*, vol. 13, no. 25, pp. 10316–10326, Dec. 2005.

[6] V. F. Rodriguez-Esquerre, H. E. Hernández-Figueroa, and M. Koshiba, "Modeling of complex structures devices and applications," in *Telecommunications: Advances and Trends in Transmission, Networking and Applications*, C. C. Cavalcante, R. F. Colares, and P. C. Barbosa, Eds. Fortaleza, Brazil: Univ. Fortaleza Press, 2006, ch. 8, pp. 173–187.

[7] M.-C. Lin and R.-F. Jao, "Finite element analysis of photon density of states for 2-D photonic crystals with in-plane light propagation," *Opt. Exp.*, vol. 15, no. 1, pp. 207–218, Jan. 2007.

[8] R. L. Haupt and D. H. Werner, *Genetic Algorithms in Electromagnetics*. New York: Wiley, 2007.

[9] S. Preble, M. Lipson, and H. Lipson, "2-D photonic crystals designed by evolutionary algorithms," *Appl. Phys. Lett.*, vol. 86, no. 6, pp. 061111-1–061111-3, Feb. 2005.

[10] G. N. Malheiros-Silveira and V. F. Rodríguez-Esquerre, "Photonic crystal band gap optimization by genetic algorithms," in *Proc. IMOC SBMO/IEEE MTT-S Int. Microw. Optoelectron. Conf.*, Salvador, Brazil, Oct.–Nov. 2007, pp. 734–737.

[11] M. Marrone, V. F. Rodríguez-Esquerre, and H. E. Hernández-Figueroa, "A novel numerical approach for the analysis of 2-D photonics crystals: The cell method," *Opt. Exp.*, vol. 10, no. 22, pp. 1299–1304, 2002.

[12] F. Quiñónez, J. W. Menezes, L. Cescato, V. F. Rodríguez-Esquerre, H. Hernández-Figueroa, and R. D. Mansano, "Band gap of hexagonal 2-D photonic crystals with elliptical holes recorded by interference lithography," *Opt. Exp.*, vol. 14, no. 11, pp. 4873–4879, May 2006.

[13] Y. Shi, "A compact polarization beam splitter based on a multimode photonic crystal waveguide with an internal photonic crystal section," *Progress Electromagn. Res.*, vol. 103, pp. 393–401, 2010.

[14] M. Mitchell, *An Introduction to Genetic Algorithm*. Cambridge, MA: MIT Press, 1996.

Gilliard Nardel Malheiros-Silveira was born in Caetité-BA, Brazil, in 1980. He received the B.Sc. degree in system analysis from the State University of Bahia, Salvador, Brazil, in 2007, the B.Sc. degree in electrical engineering from the Federal Institute of Bahia, Salvador, in 2008, and the M.Sc. degree in electrical engineering from the University of Campinas (UNICAMP), Sao Paulo, Brazil, in 2010. Currently, he is working toward the Ph.D. degree in electrical engineering at the Department of Microwaves and Optics, UNICAMP.

He is author and co-author of 2 papers in international journals and 8 papers in international conferences. His current research interests include topics related to photonics, radio frequency devices, and natural computing.

Vitaly Félix Rodríguez-Esquerre was born in Peru on February 4, 1973. He received the B.S. degree in electronic engineering from the University Antenor Orrego, Trujillo, Peru, in 1994, and the M.Sc. and Ph.D. degrees in electrical engineering from the University of Campinas (UNICAMP), Sao Paulo, Brazil, in 1998 and 2003, respectively.

He was a Post-Doctoral Research Fellow at the Division of Media and Network Technologies, Hokkaido University, Sapporo, Japan, from 2003 to 2005, and he also was a Post-Doctoral Research Fellow at the Department of Microwaves and Optics, UNICAMP, from 2005 to February 2006. He was an Adjunct Professor at the Department of Electrical-Electronical Technology, Federal Center of Technological Education in Bahia, Salvador, Brazil, from February 2006 to December 2009. Currently, he is an Adjunct Professor at the Department of Electrical Engineering, Federal University of Bahia, Salvador. He is the author and co-author of 11 papers in international journals, one book chapter, and more than 40 papers in international conferences. His current research interests include numerical methods such as the finite element and the finite difference methods for modal and propagation analysis of electromagnetic fields in conventional and photonic crystal integrated optics waveguides, metallo-dielectric nanostructures and metamaterials, integrated optics, and optical fibers.

Hugo E. Hernández-Figueroa (M'94–SM'96) received the B.Sc. in electrical engineering from the Federal University of Rio Grande do Sul, Porto Alegre, Brazil, in 1983, the M.Sc. degree in electrical engineering in 1986, and the M.Sc. degree in applied mathematics and computer science in 1988, both from the Pontifical Catholic University of Rio de Janeiro, Rio de Janeiro, Brazil. He received the Ph.D. degree in physics from Imperial College of Science, Technology and Medicine, University of London, London, U.K., in 1992.

He joined as an Assistant Professor in the Department of Microwaves and Optics (DMO), School of Electrical and Computer Engineering, University of Campinas, Sao Paulo, Brazil, in 1995, after spending two years as a Fellow with the Department of Electronic and Electrical Engineering, University College London, London. In 2005, he became a Full Professor and since 2006, he has been DMO's head. He has published over 80 papers in renowned journals and over 170 international conference papers. He is Co-Editor of the book *Localized Waves: Theory and Applications* (Wiley and Sons, 2008). He is also involved on research projects dealing with information technology applied to technology-based education. His current research interests include a wide variety of wave electromagnetic phenomena and applications mainly in photonics and microwaves.

Prof. Hernández-Figueroa has been very active with the IEEE Photonics Society, Microwave Theory and Techniques Society, Education Society, and the Optical Society of America (OSA) for the last 16 years, acting as organizer for several international conferences, guest editor for special issues, an AdCom member, and a Chapter Chair. He is a Fellow of OSA. Since 2001, he has been a member of the Editorial Board of the IEEE TRANSACTIONS ON MICROWAVE, THEORY AND TECHNIQUES. He has been an Associate Editor of the IEEE OPTO-ELECTRONICS, the IEEE INTEGRATED OPTICS, and the OSA Journal of Lightwave Technology from January 2004 to December 2009. He was the General Co-Chair of the OSA Integrated Photonics and Nanophotonics Research and Applications 2008 topical meeting. He was a recipient of the IEEE Third Millennium Medal in 2000.